Polyimide Thermal Micro Actuator

Arpys Arevalo[*1] and Ian G. Foulds[1, 2]
[1]King Abdullah University of Science and Technology
Computer, Electrical and Mathematical Sciences and Engineering Division (CEMSE)
[2]The University of British Columbia, School of Engineering, Okanagan Campus
*Corresponding author: Thuwal 23955-6900, Kingdom of Saudi Arabia, arpys.arevalo@kaust.edu.sa

Abstract: This paper presents the simulation of a chevron thermal actuator using Polyimide as the structural material. Joule heating is simulated in COMSOL for the electro-thermal micro actuator. The aim is to choose the optimal design parameters to get the largest possible in-plane displacement. The comparison between the different possible configurations will reveal the optimal parameters for the longest displacement. Our current micro fabrication process allows the actuator to use different metal configurations and choosing the best one is the goals. Generating heat in the actuator can change the material properties of polyimide and the original structure can be deformed without being able to come back to its original form. Polyimide has a decomposition temperature of 400˚. Therefore, we are interested in the maximum temperature in the micro actuator.

Keywords: Thermal actuator, chevron actuator, MEMS, Polyimide.

1. Introduction

A common bent beam chevron actuator is used in order to produce displacement in a particular in plane direction. By using its original shape, the structure amplifies the thermal expansion of the structure material. In this work we expect also a bimorph effect, because we will be using different materials to generate the in plane displacement. The required heat is generated by joule heating [1-4]. This work differs in the materials typically used. Polysilicon has been used in other works [1], because it gets doped and can be used as an electrical conductor. Due to its good coefficient of thermal conductivity is an attractive material to be used for this purpose. In our case, we are trying to generate similar displacements as in [1], while using different material configuration. Electro thermal micro actuators are able to produce higher forces at low electrical potential input in comparison to electrostatic actuators, but the trade off is in its higher power consumption [5,6]. Such devices have been used in a variety of different applications like micro-motors [7] and micro mechanical switches [8], amongst other [9-12]. Figure 1 shows an SEM image of a chevron actuator mounted on a polyimide plate.

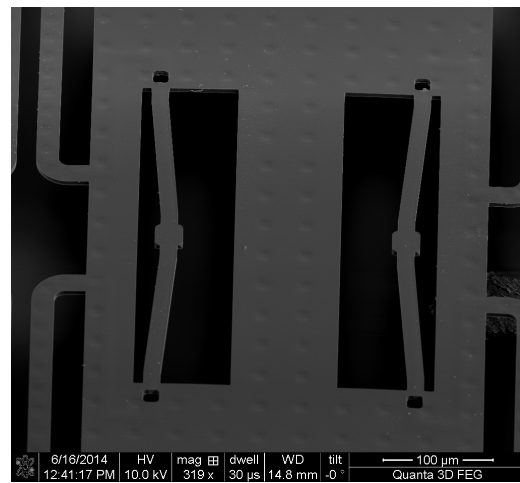

Figure 1. SEM of two opposed chevron micro actuators mounted on a polyimide plate.

According to [1], the total displacement of the chevron actuator can be increased by design. Figure 2 shows a top view of a chevron actuator and its design characteristics.

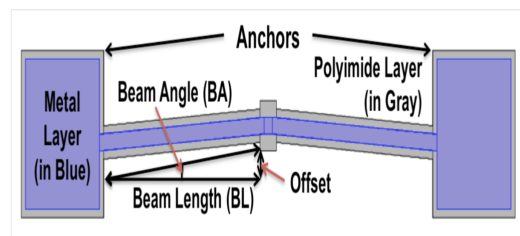

Figure 2. Chevron actuator design parameters.

If the beam angle is decreased the total displacement is increased, but for very short angles the device performance is affected having unpredictable motion. One of the results we are interested in is the z-axis displacement because our device is prone to deflect upward or downwards, due to the inherited bimorph effect

caused by different material layers used in the process. In the next section, the device's design is described.

2. Structure Design

The chevron actuator is a type of bending-beam micro actuator. The structure can be defined with the parameters shown in Figure 2: Beam Length (BL), Beam Angle (BA), Offset (OF) and the Beam Width (BW). In Figure 3, the rest of the chevron features are shown.

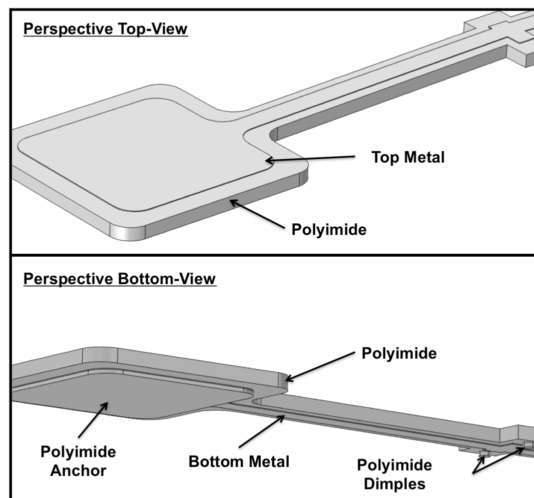

Figure 3. Top & Bottom view: left side of a chevron micro-actuator, showing its features.

When a voltage is applied between both ends of a metal layer heat is generated and the beams heat up and expand. Due to the chevron shape the displacement is guided in plane, rather than buckling the beam upwards in the case of a straight horizontal beam with no beam angle (BA = 0).

3. Chevron Micro Actuator Simulation

The 3D model was constructed from the bottom to the top of the structure starting with the anchors, which on a chip would be attached to the substrate. Because the device is symmetrical, as shown above in Figure 2, the device was modeled by drawing half of it in a work plane and then mirrored. Four work planes were used, one for the anchors and dimples, one for the bottom metal, one more for the structural layer and the last one for the top metal. All the structure was parameterized so that we could benefit of testing different geometries just by varying the parameter's dimension. Each work plane was located at different z-axis location: anchors at z = 0, bottom metal at z = 1.65, structural polyimide layer at z = 2 and top metal layer at z = 8. After building all the drawings, each work plane was extruded with their assigned layer thickness, Table 1 shows materials thicknesses.

Table 1: Layer Thicknesses

Layer	Material	Thickness
Anchors	Polyimide	2 µm
Dimples	Polyimide	2 µm
Bottom Metal	Gold	350 nm
Structural	Polyimide	6 µm
Top Metal	Nickel	350 nm

The simulation was done using COMSOL 4.4. The Electro Mechanics Module was selected because of the coupled physics considered for our problem. Our limiting factor regarding temperature was the polyimide layer because the material' glass temperature is at 360˚ C and its decomposition temperature at approximately 620˚ C [13], according to the material process guide. That means that the material will probably deform permanently if the temperature reaches its glass temperature and wont return to its original position decreasing its total displacement capability. If the material reaches or passes its decomposition temperature the organic material will become ash on the chip and no elastic properties would exit in the structure whatsoever. Therefore, we need to pay attention to the heat generated across the structure.

The model uses the material properties listed in Table 2 for the Joule Heating Model equations. The model is set to couple the involved physics phenomena in only one way, by

assuming constant materials properties. This means that the electric current through the actuator heats up the material, but the electric current is not affected by the increase in temperature of the device.

Table 2: Used Materials Properties

Gold		
Property	**Name**	**Value**
Electrical Conductivity	σ	45.6e6[S/m]
Relative permeability	ε_r	6.9
Thermal conductivity	κ	317[W/(m*K)]
Density	ρ	19300[kg/m^3]
Heat capacity	C_p	129[J/(kg*K)]
Nickel		
Electrical Conductivity	σ	13.8e6[S/m]
Relative permeability	ε_r	17.305
Thermal conductivity	κ	90.7[W/(m*K)]
Density	ρ	8900[kg/m^3]
Heat capacity	C_p	445[J/(kg*K)]
Polyimide		
Electrical Conductivity	σ	1.5e17 Ωcm
Relative permeability	ε_r	2.9
Thermal conductivity	κ	0.15[W/(m*K)]
Density	ρ	1300[kg/m^3]
Heat capacity	C_p	1100[J/(kg*K)]

For the boundary conditions three coupled physics interact between each other. In the Structural Mechanics physics, the anchors are given a fixed constraint boundary condition as a domain as shown in Figure 4a. The dimples features are given a Roller boundary condition to their bottom face, so that the device can slide along the XY plane without displacing in the z-axis, the dimples are located in the middle of the chevron as shown in Figure 4b. The rest of the faces are set to the free boundary condition.

In the Heat Transfer in Solids physics, both bottom faces of the anchors and the dimples are set to a room temperature of 20˚ C, which is the temperature of the substrate they would be attached to. The rest of the faces of the structure are set to a convective heat boundary condition, using the heat flux option for an external natural convection simulating the temperature of the air around the device with a wall height of 1 meter.

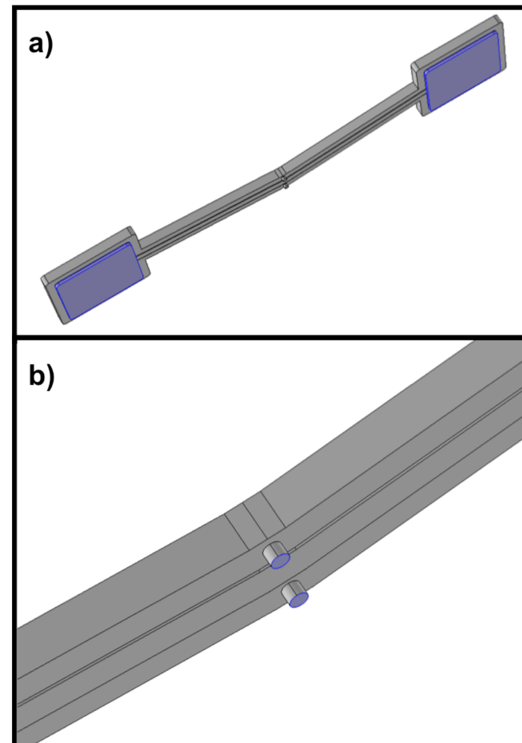

Figure 4. Structural Mechanics boundary conditions, a) anchors domain have a fixed constraint boundary condition; b) dimples bottom faces are set to a roller boundary condition.

For the Electric Currents physics a terminal and a ground was define to pass current through the conductive material and to simulate the joule heating. After all the boundaries were properly selected a first simulation was run to test the settings. Figure 5 shows a simulation of a chevron actuator. The displacement is fixed to move in the XY plane and fixed in z = 0, due to the roller boundary condition.

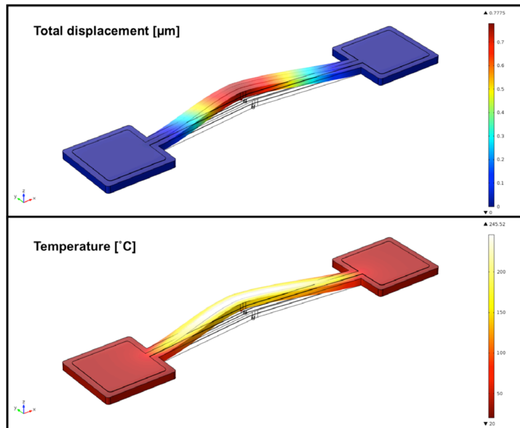

Figure 5. Simulation of a chevron thermal actuator with configuration BA: 6 BL:100 and BW:5. Applied voltage 0.3 V, maximum displacement 0.7775 µm, maximum temperature (bottom image) is 245.52˚C.

As shown in Figure 5 above, short beams reach high temperatures with really low voltage applied. This was expected because of the thin and short metal layer. By increasing the length and width of the beam the device is able to handle more voltage, which is needed to generate more displacement.

If we remove the roller boundary condition, COMSOL displays the bending of the beam towards the surface as shown in Figure 6, where the result is being exaggerated by 10 times to be able to appreciate the bent.

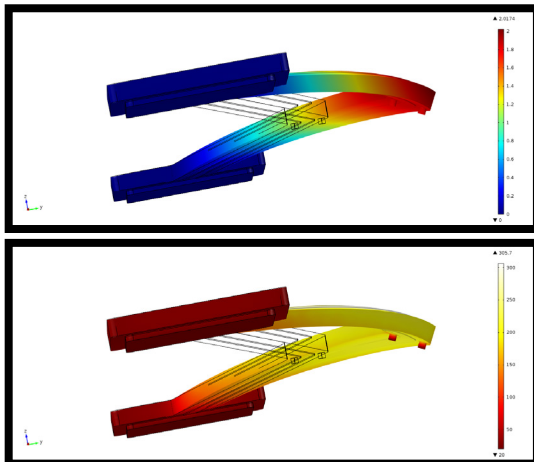

Figure 6. Simulation of a chevron thermal actuator with configuration BA: 12 BL:200 and BW:5. Applied voltage 0.6 V, maximum displacement 2.0174 µm, maximum temperature (bottom image) is 305.7˚C.

Finally a comparison between how much voltage can be applied for the maximum temperature that the device can handle is shown in Figure 7.

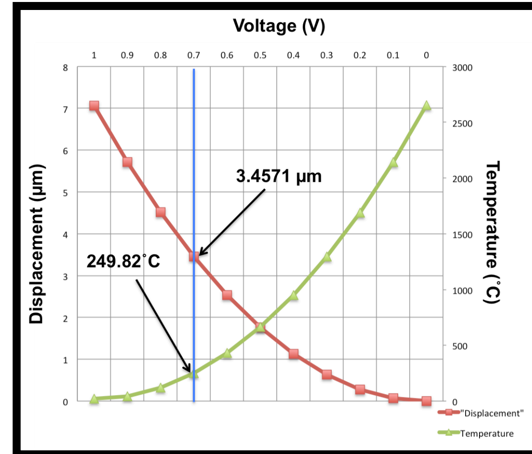

Figure 5. Graph showing the admissible voltage to actuate a chevron configuration BA: 6 BL: 100 and BW: 5.

In the figure above it can be seen that the safest voltage input to the device is approximately 0.7 V, where the device would give about 3.5µm of total displacement and the temperature would be 100 ˚C lower than the glass transition temperature of the polyimide.

The effect of applying voltage on the bottom metal layer was on helping the buckling effect while removing the roller boundary condition. We should look at this effect with experimentation and compare if the ratio between metals is the appropriate. From experience we are aware that the by depositing different ratios of thickness on the structural layer helps removing the curvature generated through all the fabrication steps.

8. Conclusions

From the simulations results we could see that there are a few disadvantages to implement in plane thermal actuators with our process, due to the bimorph effect produced by the different layers used for the devices. Part of the displacement is focused towards or opposite to the substrate, which could potentially create a miss-match when trying to interact with other structures on the wafer. Also, by displacing

towards the substrate an electrical short can be generated and burn the device. In general the chevron actuators would have a lower displacement using our fabrication process than using POLYMUMPs [1] for example. Nevertheless, large displacements out of plane can be produced and this effect can be implemented in a different configuration for out-of-plane micro-structures [14-17], and potentially be used with our micro fabrication process, for the motion of sensors and actuators such as antennas [14] or micro mirrors amongst others. The next step is to fabricate these devices and characterize them to compare with the simulation results. Also we are generating new designs to take advantage of the bimorph effect for a possible controllable micro mirror.

9. References

1. Ehab Rawasdeh, A. Karam, I G Foulds, "Characterization of Kink Actuators as Compared to Traditional Chevron Shaped Bent-Beam Electrothermal Actuators", Micromachines. (2012)
2. Cragun, R.; Howell, L.L. Linear thermomechanical microactuator. In Proccedings of the ASME International Mechanical Engineering Congress and Exposition, Microelectromechanical Systems (MEMS), Nashville, TN, USA, 14–19 November 1999; pp. 181–188. (1999)
3. Jae-Sung, P.; Chu, L.L.; Oliver, A.D.; Gianchandani, Y.B. Bent-beam electrothermal actuators —Part II: Linear and rotary microengines. J. Microelectromechan. Syst. 2001, 10, 255–262. (2001)
4. Sinclair, M.J. A high force low area MEMS thermal actuator. In Proccedings of the seventh Intersociety Conference on Thermal and Thermomechanical Phenomena in Electronic Systems, Las Vegas, NV, USA, 23–26 May 2000; p. 132. (2000)
5. Varona, J.; Tecpoyotl-Torres, M.; Hamoui, A.A. Design of MEMS vertical-horizontal chevron thermal actuators. Sens. Actuat. A-Phys. pp. 127–130. (2009)
6. Long, Q.; Jae-Sung, P.; Gianchandani, Y.B. Bent-beam electrothermal actuators—Part I: Single beam and cascaded devices. J. Microelectromechan. Syst. 10, 247–254. (2001)
7. Varona, J.; Tecpoyotl-Torres, M.; Escobedo-Alatorre, J.; Hamoui, A.A. Design and fabrication of a MEMS thermal actuator for 3D optical switching applications. In Proccedings of the Digest of the IEEE/LEOS Summer Topical Meetings, Acapulco, Mexico, 21–23 July 2008; pp. 31–32. (2008)
8. Jae-Sung, P.; Chu, L.L.; Oliver, A.D.; Gianchandani, Y.B. Bent-beam electrothermal actuators—Part II: Linear and rotary microengines. J. Microelectromechan. Syst. 2001, 10, 255–262. (2001)
9. Gravier, S.; Coulombier, M.; Safi, A.; Andre, N.; Boe, A.; Raskin, J.P.; Pardoen, T. New on-chip nanomechanical testing laboratory—applications to aluminum and polysilicon thin films. J. Microelectromechan. Syst. 2009, 18, 555–569. (2009)
10. Daneshmand, M.; Fouladi, S.; Mansour, R.R.; Lisi, M.; Stajcer, T. Thermally actuated latching RF MEMS switch and its characteristics. IEEE Trans. Microwave Theory 2009, 57, 3229–3238. (2009)
11. Unamuno, A.; Uttamchandani, D. MEMS variable optical attenuator with vernier latching mechanism. IEEE Photonic Technol. Lett. 2006, 18, 88–90. (2006)
12. Wen-Chih, C.; Chia-Yu, W.; Chengkuo, L. Bi-directional movable latched micromechanism using one-directional movable chevron electrothermal actuators for switch and relay applications. In Proccedings of the Microprocesses and Nanotechnology Conference, Tokyo, Japan, 29–31 October 2003; pp. 180–181. (2003)
13. HD Microsystems, "PI-2600 Series – Low Stress Applications", Technical Information. [http://hdmicrosystems.com/HDMicroSystems/en_US/pdf/PI-2600_ProcessGuide.pdf](2009)
14. L. Marnat, A. A. A. Carreno et al., "New Movable Plate for Efficient Millimeter Wave Vertical on-Chip Antenna," IEEE Transactions on Antennas and Propagation, vol. 61, pp. 1608-1615, April 2013. (2013)
15. A. Alfadhel, A. A. A. Carreno et al., "Three-Axis Magnetic Field Induction Sensor Realized on Buckled Cantilever Plate," Ieee Transactions on Magnetics, vol. 49, pp. 4144- 4147. (2013)
16. A. A. A. Carreno et al., "µHeater on a Buckled Cantilever Plate for Gas Sensor Applications", COMSOL Conference, Milan, Italy. (2012)
17. A. A. A. Carreno et al., "Optimized Cantilever-to-Anchor Configurations of Buckled Cantilever Plate Structures for Transducer Applications", COMSOL Conference, Milan, Italy. (2012)